DIMM sampling of the "seeing" at Kryonerion

by D. Mislis[1], E.T. Harlaftis[2,†], D. Buckley[3], K. Gazeas[4], K. Stathoulis[5], G. Dimou[6], J.-H. Seiradakis[1]

1. *Department of Physics, Section of Astrophysics, Astronomy and Mechanics, University of Thessaloniki, Thessaloniki - GR 54124, Greece*
2. *Institute of Space Applications and Remote Sensing, National Observatory of Athens, P.O. Box 20048, Athens -11810*
3. *South African Astronomical Observatory, PO Box 9, Observatory 7935, Cape Town, South Africa*
4. *Department of Physics, Section of Astrophysics, Astronomy and Mechanics, University of Athens, Zografos, Athens – GR 15783, Greece*
5. *Intracom IT Services, 19.3 km Markopoulou Ave., Peania, GR-19002 Athens, Greece*
6. *Institute of Astronomy & Astrophysics, National Observatory of Athens, P.O. Box 20048, Athens –11810, Greece*

† *In memoriam. Passed away on 13 February 2005*

Abstract

We present a test-study of the "seeing" at the Kryonerion Station of the National Observatory of Athens. We used a Differential Image Motion Monitor (DIMM) during July and October 2002 and find a median "seeing" of 0.68 arcseconds and 1.42 arcseconds, respectively. We also compared the technique against the Hartmann-version of the ESO-type DIMM method and found similar results within 0.05 arcseconds. For some reason, which is under investigation by international teams, the measurements of our ESO-type DIMM are underestimated by ~10% compared to ESO-standard DIMM measurements. Simultaneous ESO-type DIMM measurements and standard gauss-fitting-technique measurements, taken with the Kryonerion 1.2m telescope (inside the dome) indicate that the "seeing", as measured by the telescope is by ~1 arcsecond larger. The above tests were performed in order to calibrate, test and make a brief sampling of the "seeing" at the Kryonerion Station with the aim to move eventually the equipment to the Helmos Station –the site of the new 2.3m ARISTARCHOS telescope– for a long-term "seeing" monitoring. As a by-product of this project, a new DIMM station became operational at Mt. Holomon, in the premises of the University of Thessaloniki, in 2004.

1. Introduction

The new station for the 2.3m telescope of the National Observatory of Athens lies at the peak of the 2.3km Helmos mountain, close to the historic-town of Kalavryta in North Peloponese (longitude 22°13' E and latitude 37°59' N). The site characterization of the Helmos Station was immediately one of the concerns for developing further international collaboration and exploiting in full the scientific potential of the new site. In particular, addressing concerns within the OPTICON network regarding the unknown properties of the Helmos night sky, we took initiative to put together a package with the aim to address at least the "seeing" characteristics by setting-up a portable differential image motion monitor (DIMM; Sarazin & Roddier 1990; Tokovinik 2002). Previous measurements of the site "seeing", using the stellar trail technique, were indicating a median seeing as good as 0.7 arcseconds from a sample of 30 winter nights (Sinachopoulos et al. 2000), though this technique is known to be instrument-dependent. As a matter of interest, the stellar trail technique gave similar relative "seeing" measurements between Calar Alto and Mount Parnon (Pyrgaki, 1.8 km) at south-east Peloponnese (longitude 22°.6 E and latitude 37°.2 N) back in the 70's (Birkle et al. 1976). The DIMM method removes every error due to bad tracking, wind or mirror blotches by using a differential measurement of the stellar image motion (through two apertures). Given the minimal resources available, we adopted a portable-version of DIMM, leaving for the next stage the construction of a fixed tower.

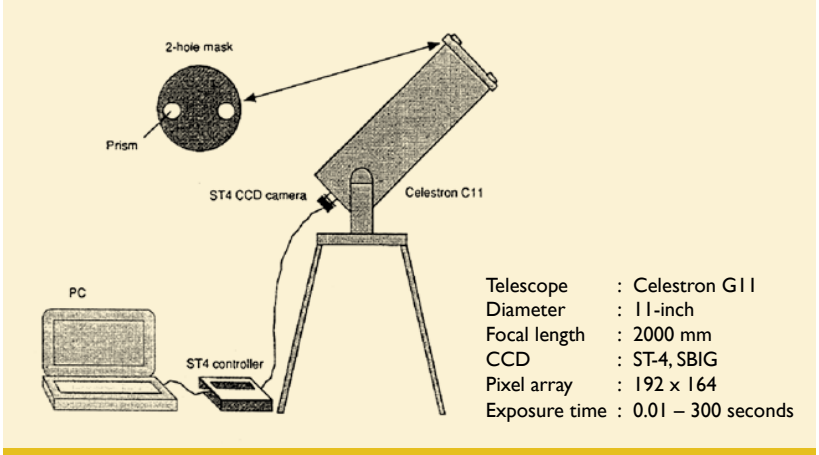

Figure 1. The "SAAO DIMM" equipment

2. Instrumentation and set-up

All major Observatories had set-up such "seeing" measuring instruments in the 90's and therefore ample expertise was at hand in the 00's. For example, the IAC DIMM at La Palma (Vernin & Munoz-Tunon 1995), the ING DIMM at La Palma (Wilson et al. 1999), and the Mount Stromlo portable DIMM (Wood, Rodgers & Russell, 1995). SAAO also built an identical set-up for the SALT site testing at Sutherland (Erasmus 2000). The lat-

ter was cross-calibrated with the ESO-standard DIMM (Sarazin & Roddier 1990) at various sites and only recently (end of 2004) it was confirmed that it gives a small under-estimate of ~10% (under investigation but most likely due to software pixel sampling). This portable ESO-type DIMM ("SAAO DIMM" – Fig. 1) was then duplicated and used at Kryonerion, NOA. After the Sutherland site-testing finished, some core equipment (CCD-Celestron telescope, interface, mask, ST-4 CCD) was shipped to NOA. The equipment, hardware and software was assembled and tested at the Kryonerion Station (height 898±5 m, longitude 22° 37' 06" and latitude 37° 58' 18"), due to lack of infrastructure and logistics at the Helmos Station. Here, we describe the test measurements we took at Kryonerion during the summer season in 2002. It was envisioned, then, to take up the equipment at a purpose-built hut at the Helmos Station and monitor the "seeing" for one full year.

The technical equipment we used included a 11-inch CELESTRON telescope, a ST-4 SBIG CCD camera and a front-edge telescope mask (Fig. 2). The mask had two apertures, and one of them had a prism that displaced the direct light from the star by ~20 arcseconds. This meant that when we observed a star we were observing two spots from the same source whose differential motion is given as variance errors in the x and y-axis on the CCD chip (Sarazin & Roddier 1990):

$$\sigma_X^2 = 2 \cdot \lambda^2 \cdot r_{oX}^{-5/3} \cdot (0.179 \cdot D^{-1/3} - 0.0968 \cdot d^{-1/3}) \quad (1)$$

$$\sigma_Y^2 = 2 \cdot \lambda^2 \cdot r_{oY}^{-X/3} \cdot (0.179 \cdot D^{-1/3} - 0.1450 \cdot d^{-1/3}) \quad (2)$$

where λ is the wavelength, r_o is the Fried parameter (average turbulent cell), D the diameter of apertures and d the distance of the apertures.

The set-up is displayed in Fig. 1 and the instrumentation is described in detail at Wood et al. (1995). Using the CCD's turbo-pascal software, we measure the variance of the relative positions of the two spots very precisely in both axes. Then, from equations (1) and (2) we can calculate the Fried parameter and from there, the "seeing" (Vernin & Munoz-Tunon 1995; Fried 1965):

$$Seeing(FWHM) = 0.98 \cdot \frac{\lambda}{r_o} \quad (3)$$

3. Seeing Methods and airmass calibration: Results

In addition to the mask/prism DIMM, there is a simpler method just using the Hartmann mask (H-DIMM; Bally et al. 1996) which we also used for comparison. This method uses the same equipment as the SAAO DIMM, but instead of using a prism we just defocus the telescope by a few millimetres to create two image spots. The distance to defocus is given by

$$X = \frac{F}{D} \cdot P \quad (4)$$

where X is distance from the focus in mm, F is the telescope's focal length in mm, P is the pixel size in mm and D is the distance between the two apertures. We typically found that the de-focusing length needed was only 1.3 mm. Our purpose was to check if the H-DIMM method gives the same results as the SAAO DIMM method. We made two masks, one with a prism (prism-DIMM method) and one without (H-DIMM method). During the test observations, the masks were changed every ten minutes. The result of our observations on a photometric night (28 May 2003), using the star α Boo, is shown in Fig. 3, proving that the two methods give identical results within a 0.05 arcseconds accuracy (prism-DIMM Seeing Average = 0.98 arcseconds and H-DIMM Seeing Average = 1.00 arcseconds).

Every time that we measure the seeing from a star, we need to calibrate the data for the changing airmass. This is necessary because "seeing" is a function of the air mass, therefore it is also a function of the star's altitude. For this reason we normalized all measurements at the air mass minimum (zenith). To do that we use equation 5 (Humphries et al. 1984),

$$S \propto S_o \cdot a^{-0.6} \quad (6)$$

where S is the calibrated value at zenith and S_o the "seeing" at airmass a. In the figures following (Fig. 4) we give the corrected "seeing" measurements during our test DIMM observations in July and October 2002.

Figure 2. The CELESTRON telescope and PC driving the "seeing" measurements, next to the small enclosure built to protect the telescope from weather. At the background, the 1.2m telescope dome of the Kryonerion Observatory can be seen.

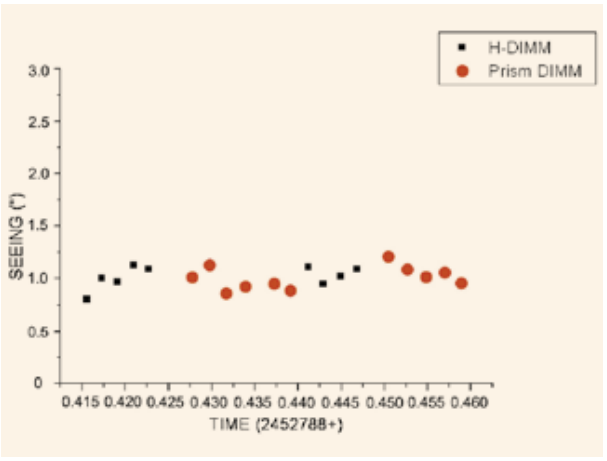

Figure 3. Prism-DIMM vs. H-DIMM. 28/05/2003, α Boo

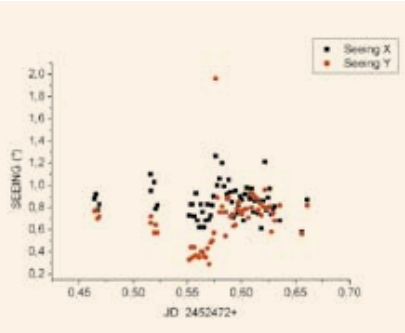

Figure 4a. 16/07/2002, α Lyr

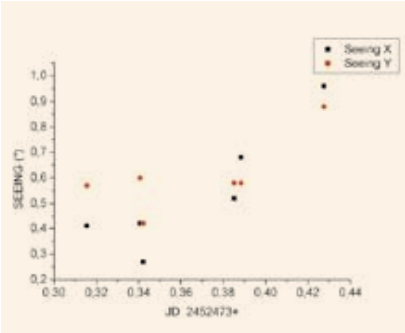

Figure 4b. 17/07/2002, γ Cyg

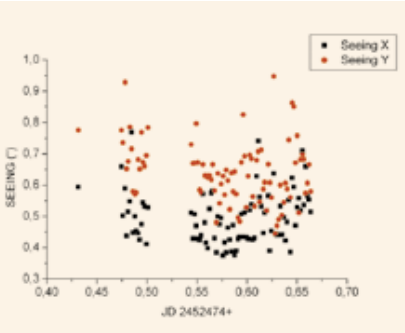

Figure 4c. 18/07/2002, α Lyr

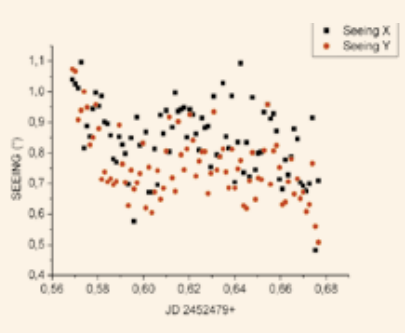

Figure 4d. 23/07/2002, α Lyr

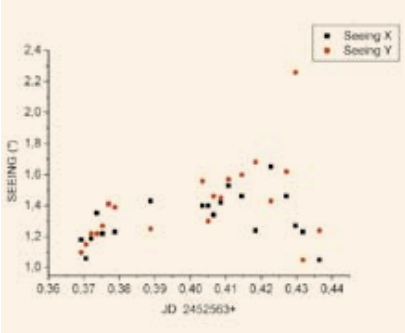

Figure 4d. 23/07/2002, α Lyr

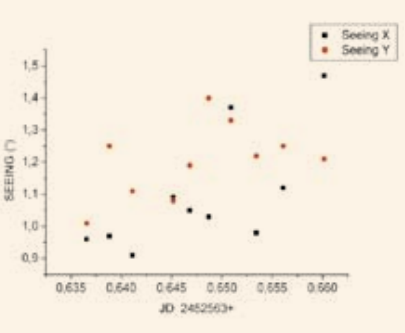

Figure 4f. 15/10/2002, β Ori

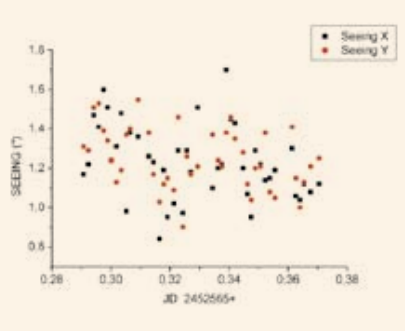

Figure 4g. 17/10/2002, α Lyr

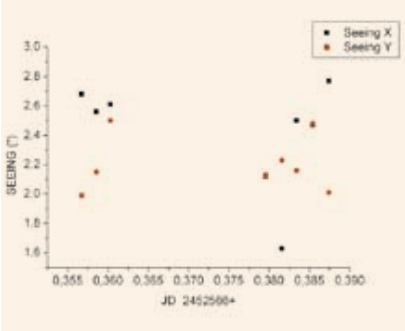

Figure 4h. 18/10/2002, α Cyg

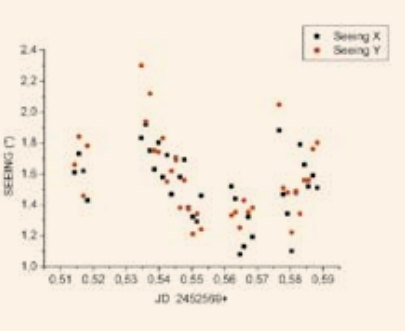

Figure 4i. 21/10/2002, β Ori

From the SAAO DIMM measurements we have:

Table 1: Seeing measurements at Kryonerion Station

Date	Seeing x-axis (arcsec)	Seeing y-axis (arcsec)	Standard Deviation X-axis	Standard Deviation Y-axis	Median "seeing" (arcsec)	Average "seeing" (arcsec)	Standard Deviation of Average
16/07/2002	0.85	0.69	0.10	0.14	0.71	0.77	0.12
17/07/2002	0.54	0.61	0.15	0.09	0.61	0.58	0.12
18/07/2002	1.60	1.42	0.30	0.27	0.80	1.51	0.29
23/07/2002	0.48	0.61	0.10	0.20	0.68	0.55	0.22
13/10/2002	1.69	1.64	0.28	0.19	1.60	1.67	0.24
14/10/2002	1.06	0.98	0.32	0.33	1.06	1.02	0.33
15/10/2002	1.40	1.43	0.11	0.15	1.38	1.42	0.13
16/10/2002	1.10	1.21	0.12	0.16	1.10	1.16	0.14
17/10/2002	1.23	1.25	0.13	0.11	1.33	1.24	0.12
18/10/2002	2.42	2.21	0.21	0.11	2.42	2.32	0.16
21/10/2002	1.53	1.58	0.30	0.34	1.05	1.56	0.32
Average	1.26	1.24	0.19	0.19	1.06	1.25	0.19

Using the data in Table 1, we extract the average and the median seeing value per month (Table 2).

Table 2:
Monthly seeing average at Kryonerion Station

Month (2002)	Median "Seeing" (arcsec)	Average "Seeing" (arcsec)	Standard Deviation (arcsec)
July	0.68	0.87	0.15
October	1.42	1.49	0.21

4. "Seeing" as measured through the telescope

For comparison reasons, we present "seeing" measurements obtained with star trails, using the 1.2m telescope, between 20 October – 6 November 1999 (whilst the neutron-star X-ray transient XTE J1859+226 was in outburst). The air mass has been calibrated and the results are given in Table 3 and the figures below (Fig. 5).

Table 3:
Seeing measurements with the 1.2 m Kryonerion telescope, using star trails

Date	Average "seeing" (arcsec)
20 October 1999	2.40
24 October 1999	2.00
25 October 1999	2.00
26 October 1999	2.46
29 October 1999	2.93
31 October 1999	2.39
1 November 1999	2.02
2 November 1999	2.57
3 November 1999	3.00
6 November 1999	3.50
Average	2.53
Standard Deviation	0.47

5. Discussion

We constructed a prism DIMM setup at Kryonerion Station, based on the SAAO DIMM. The setup was tested at Kryonerion, a well known observing site, in order to use it later at the new Helmos site. We also constructed and tested an H-DIMM setup. The two methods gave almost identical results. The "seeing" at Kryonerion (using the above setups), from a sample of nights in October 2002, was 1.42 arcseconds (median) or 1.49±0.21 arcseconds (average). For comparison, the average "seeing" measurements made with the 1.2 m telescope (from inside the dome), in October/November 1999, was 2.53 arcseconds with a standard deviation of 0.47 arcseconds. The "seeing" at Kryonerion from a sample of nights in July 2002 was 0.68 arcseconds (median) or 0.87±0.15 arcseconds (average). Note that there is an underestimate of ~10% in the above measurements, which were based on the SAAO DIMM, as mentioned above. DIMM measurements, taken outside and measurements taken with the Kryonerion 1.2 m telescope (from inside the dome) gave ~1 arcsecond and ~2 arcseconds, respectively, on 1 July 2002. Therefore, the typical difference between the seeing value inside the dome and outside the dome is approximately 1.0 arcseconds. This prompted a follow-up analysis of the optical system of the telescope (Worswick S., Harlaftis, E.T., Dimou, G., this volume). Some of the equipment has been moved to Mt. Holomon Station of the University of Thessaloniki where a DIMM setup is operating since 2004.

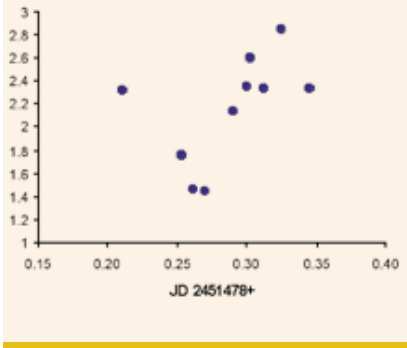

Figure 5a. 26/10/1999, XTE J1859+226

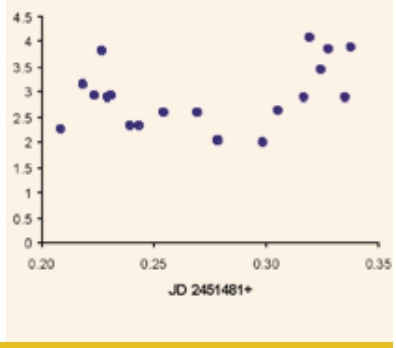

Figure 5b. 29/10/1999, XTE J1859+226

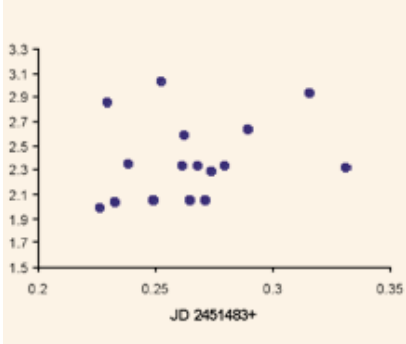

Figure 5c. 31/10/1999, XTE J1859+226

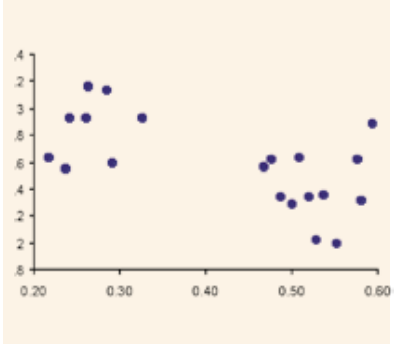

Figure 5d. 02/11/1999, XTE J1859+226

Acknowledgements:

We would like to thank Neil O'Mahony and David M. Russell for useful discussion on DIMM aspects.

References

Bally, J., Theil, D., Billawala, Y., Potter, D., Loewenstein, R. F., Mrozek, F., Lloyd, J. P., "A Hartman Differential Image Motion Monitor (H – DIMM) for Atmos Turbulence Characterisation", 1996, A&A 13, 22-27

Birkle, K., Elsasser H., Neckel, Th., Schnur, G., 1976, A &A, 46, 397

Erasmus, A., "Meteorological Characterization of the Sutherland Astronomical Observatory and Evaluation of Candidate Sites for the Southern African Large telescope", 2000, SALT technical report, SAAO

Fried, D. L., 1965, J. Opt. Soc. Am., 55, 1427

Humphries. C. M., Reddish V. C., Walshaw, D. J., "Cost scaling laws and their origin - Design strategy for on optical array telescope", 1984, IAU Colloquium 79, "Very Large Telescopes, their Instrumentation and Programs", 379

Sarazin, M., Roddier, F., "The ESO differential image motion monitor", 1990, A & A., 227, 294-300.

Tokovinik, A., "From Differential Image Motion Monitor to Seeing", 2002, PASP, 104, 760.

Vernin, J., Muñoz – Tunon, C., "Measuring Astronomical Seeing: The DA/IAC DIMM ", 1995, PASP, 107, 275

Sinachopoulos, D., Dapergolas, A, Kontizas, E, Korakitis, R., 2000, Birth and Evolution of Binary Stars, IAU Symposium No. 200, eds. B. Reipurth & H. Zinnecker, p. 180

Wilson, R.W., O'Mahony, N., Packham, C., Azzaro, M., 1999, MNRAS, 309, 379

Wood, P. R., Rodgers, A. W., Russell, K. S., 1995, PASA, 12, 97

The Image quality of the 1.2m telescope of the National Observatory of Athens

by Sue Worswick[1], Emilios T. Harlaftis[2,†], George Dimou[3]

1. *Observatory Optics, 1 Betony Vale, Royston, SG8 9TS, UK*
2. *Institute of Space Applications and Remote Sensing, National Observatory of Athens, P.O. Box 20048, Athens 11810, Greece*
3. *Institute of Astronomy and Astrophysics, National Observatory of Athens, P.O. Box 20048, Athens 11810, Greece*

† *In memoriam. Passed away on 13 February 2005*

Abstract

We derive f/13.6 for the 1.2m telescope of the National Observatory of Athens (image scale 0.303 arcseconds per 24 μm pixel) and find that the image quality is dominated by large spherical aberration (2.5 arcseconds for 100% encircled energy). Sub-arcsecond "seeing" convolved with the telescope's optics cannot deliver better image quality than 1.54 arcseconds and real "seeing" is not dominated by spherical aberration for values larger than 3 arcseconds. The combined mirror polishing error is 0.49 arcseconds for 95% encircled energy. The peak to valley error on the primary mirror is 0.236 μm. Out-of-focus images indicate that the support of the mirror is not optimized causing its edge to be raised by 3 μm.

1. Introduction

The f/13.6 1.2m telescope built by Grubb Parsons in 1973 for the National Observatory of Athens resides nearby the village of Kryoneri at prefecture of Korinthia (Rovithis et al. 1999).

Summer research observations by Harlaftis et al. over the past five seasons indicate that the measured "seeing" through the telescope rarely becomes better than 2 arcseconds. DIMM measurements in 2002 showed, on the other hand, that the Kryoneri site could deliver sub-arcsecond "seeing" (Mislis et al. 2005). Thereafter, one of us instigated an optical analysis of the telescope optics in order to verify the "Optical test Reports for the 1.2m telescope for Athens" (Grubb Parsons, hereafter "GP", March 1975) and analyse the image quality. We perform two different analyses: the first is using the optical prescription as given in the "Optical test reports" (design optical system). The second is to use out-of-focus images at both sides of the focal plane (current optical system). The "ZEMAX" optical analysis tool is used throughout the report.

2. Optical Prescription

In a Cassegrain telescope the spherical aberration of the primary mirror is fully corrected by making the surface a paraboloid (conic constant k=-1). The secondary mirror operates with a virtual object, lying at the primary mirror focus, and a finite image lying at the Cassegrain focus. These conjugates define a hyperboloid. The mirror separation required is purely determined by the radii of curvature of the two mirrors and the position of the final Cassegrain focus with respect to the primary mirror surface. The hyperboloidal secondary should have a conic constant (aspheric figuring) that corrects the spherical aberration for the mirror separation and back focal distance that is used on the telescope mount.

Thereafter, the inherent image quality of the telescope optical prescription can be assessed by knowing the conic constant and the mirror separation. The surfaces of the primary and secondary mirrors are defined by the radii of curvature and the form constants (b_2) in the GP report to give the conic constant for a surface $k=-(b_2)^2$ (Table 1).

The manufactured value for k for the secondary mirror is further confirmed by the wavefront error (0.0025 waves or ~1.5nm) obtained for the null test configuration and the secondary mirror parameters given in the GP report.

An estimate of the back focal distance (1001.1mm) has been made by combining the distance between the front surface of the primary and the back of the mirror cell (485.4mm; Grubb Parsons drawing TA1.220) with the measured distance between the back of the mirror cell and the CCD focal plane (458+10+47.7=515.7mm). The separation between the primary and secondary mirrors is 2770.63 mm for the image behind the primary to be at 1001.1 mm. The telescope prescription is given below (Table 2); all the dimensions are in mm. "Surface" is the virtual or real surface (primary or secondary mirror) that the ray reflects to or passes through. "Radius" is the radius of curvature of the surface and "Thickness" is the distance from the surface to the next one in the system.

The image spread at the measured back focal distance is large and shows that the conic constant of the secondary mirror is not correct. The spot diagram in Figure 1 is plotted for a wavelength of 590nm (0.59 microns; consistent with

Table 1

	Radius of curvature mm	Form constant b_2	Conic constant k
Primary mirrr	7198	1.0000	–1.0000
Secondary mirror	2123	1.4358	–2.06152

Table 2: Surface Data summary

Surface	*Radius*	*Thickness*	*Glass*	*Diameter*	*Conic*
object	Infinity	Infinity		0	0
p. m.	Infinity	2800.00		1200	0
stop	–7198	–2770.632	MIRROR	1200	–1
sec. m.	–2123	2770.632	MIRROR	330	–2.06152
p.m. shell	Infinity	485.4		73.91	0
focal plane	Infinity	515.7		1200	0
image	Infinity			0.784	0

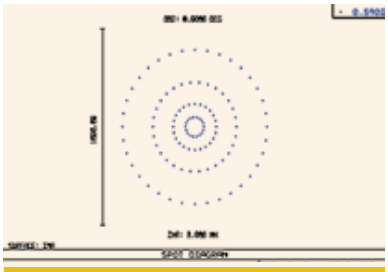

Figure 1.

GP report) and the 4 rings represent the image positions for rays at 4 different radii across the telescope aperture. The telescope can be refocused, by increasing the mirror separation by about 0.4 mm, to minimise the image spread from spherical aberration. The total spread is then contained within 208 microns (2.6 arcseconds). The 50% encircled energy is contained in a diameter of 1.51 arcseconds. The peak to valley wavefront error is reduced to about 2.3 waves (~1400nm). The manufactured value of k, –2.01652, would require the focus of the pair of mirrors to lie a further 1143 mm from the primary for the spherical aberration of the mirror combination to be zero and would yield a focal length of 20115 mm and an f-number of f/16.76.

The correct secondary conic constant for an f/13 telescope configuration would be –2.443 to yield zero spherical aberration. For a separation of 2771 mm between the primary and secondary mirrors and 1001 mm focal plane distance from the front of the primary mirror, the focal length of the telescope is 16359.8 mm and the focal ratio is f/13.63. A 7 mm movement of the secondary mirror corresponds to a 140mm movement of the Cassegrain focal plane. The f/13.6 gives an image scale of 79.3 microns per arcsecond or 0.303 arcsecond per 24 µm pixel. This is consistent with the 0.301 arcsecond per 24 µm pixel derived by Synachopoulos et al. (1999) using Hipparchos double stars (with around 15 arcsecond separation).

3. Polishing errors

A summary of the polishing errors for the primary and secondary mirrors is presented in the GP report. The primary mirror analysis, presented in the GP report, gives the following encircled energy diameter results. The secondary mirror analysis in the GP report states that the wavefront errors are of the opposite sign to those on the primary and so the spread for the two mirrors in combination will be smaller than those from the primary mirror alone (0.49 arcsecond at 95% encircled energy). These errors represent a much smaller contribution to the image spread than the effects from the incorrect conic constant for the secondary mirror. The results are given the Table 3.

The GP report gives a summary of the radial distribution of wavefront errors for the primary mirror and two profiles across the diameter of the secondary mirror. They represent the variations in mirror height, which are fitted using a polynomial distribution in order to estimate the image spread obtained by the combination of the polishing errors from both mirrors (see Figure 2). For both mirrors the RMS on the fit is of the order of 0.03 waves. The peak to valley error on the primary mirror (similar for the secondary mirror) is about 0.2 waves on the surface, which will be 0.4 waves on the wavefront because of the doubling on reflection; this is 236 nm or 0.236 microns. The test wavelength used throughout this paper and in the GP report is 590 nm. The data presented in the GP report do not provide sufficient information to produce a detailed, two dimensional, wavefront error map.

4. Out-of-focus image analysis

The current status of the focus drive on the 1.2 m telescope does not permit accurate, known, focus offsets to be applied to the secondary mirror. However it is possible to produce pairs of images with approximately equal and opposite secondary mirror offsets about the best focus position. By defocusing the image it is possible to assess whether there are any aberrations present that may be degrading the image. A pair of images was obtained on 14/09/2004, indicative of the current optical system status.

The frame size for each picture represents an area approximately 12.3x12.3 mm. The CCD frames have been binned up 2x2 yielding a pixel size of 0.048 mm. The diameter of the out-of-focus images is approximately 215 pixels (10.3 mm). This would be an equivalent of a defocus of about ±140 mm at the Cassegrain focus or ±7 mm at the secondary mirror.

The out-of-focus images show the central obstruction from the secondary mirror baffle (480 mm giving a 40% linear obstruction ratio for the telescope). The two images show a change in the relative size of the central obstruction on either side of focus, typical of spherical aberration. This has a larger diameter if it is closer to the primary (intra focal

Table 3

Encircled energy %	Primary mirror Energy diameter (arcseconds)	Combined mirrors Energy diameter (arcseconds)
80	0.46	0.34
85	0.50	0.40
95	0.58	0.49
99	0.68	
100	0.72	

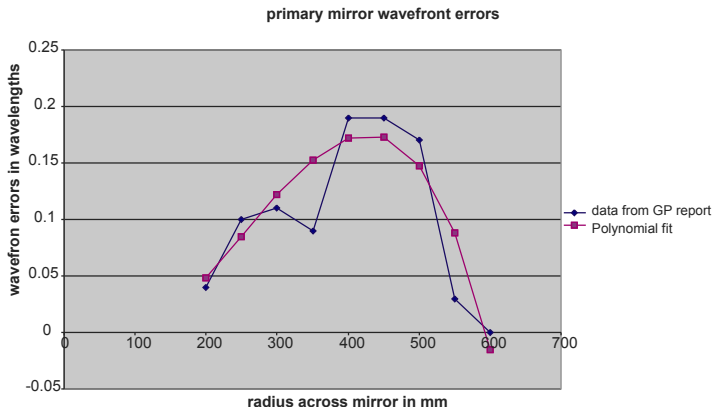

Figure 2. The radial distribution of the wavefront errors for the primary mirror.

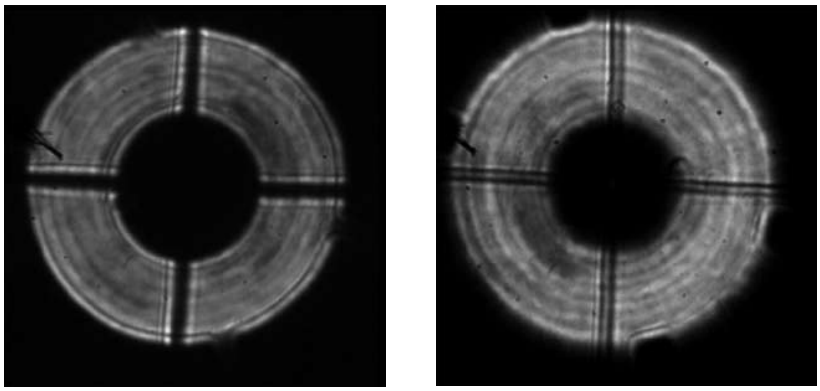

Figure 2. Intra focal image (left) and Extra focal image (right)

position) and a smaller diameter when it is away from the telescope (extra focal position).

We can estimate the amount of spherical aberration by using the relative diameters of the central obstructions of the two out-of-focus images (Wilson 1999). Both the outside and inside diameters are used of the intra and extra focal images as a consistency check. If D_I is the diameter of the central obstruction and d_I is the outer diameter for the intra focal image and D_E and d_E are the same parameters for the extra focal image. A quantity ΔD is derived which is given by

$$\Delta D = D_I - D_E\,(d_I/d_E)$$

The diameter of the best focus image for the telescope with a normalised central obstruction ratio of ε (0.4 in the case of the Kryoneri telescope) is given by

$$\Delta D/(8\varepsilon*(1-\varepsilon^2)*scale)$$

where *scale* is the image scale at the telescope focal plane in mm per arcsecond (0.0793 in the case of the 1.2m telescope). Measurements have been made in several different directions across the out-of-focus images (Table 4). The average value for ΔD is 0.48 ± 0.08 mm. This yields a best focus image spread (100% encircled energy) of 2.25 ± 0.37 arcseconds. The error in the measurements comes from the signal to noise in the exposures but also from effects around the mirror boundaries such as "seeing".

5. Models of out-of-focus images

We model the out-of-focus images produced by the telescope optical prescription (GP report) for comparison to the observed pair of the out-of-focus CCD images. The image size has been set to 12.3x12.3 mm and is divided into 256x256 pixels. Secondary mirror displacements of ±7mm have been used and the system is illuminated with a source representing a seeing disc of 1 arcsecond FWHM. The shape of the images (GP report) is in agreement with those taken on the telescope except for the sign of the spherical aberration. As the secondary mirror is moved away by 7 mm from the primary mirror the extra focal image will fall on the detector (larger obstruction diameter corresponding to negative spherical aberration). The opposite is true for the out-of-focus CCD images where the larger obstruction diameter corresponds to the secondary mirror movement towards the primary mirror (positive spherical aberration). Spherical aberration is positive for a system that has the marginal (edge of the mirror) rays coming to focus before those that lie toward the centre of the aperture. In this case the central obstruction appears larger for the intra focal CCD image. Additional pairs of out-of-focus images were obtained to confirm the secondary mirror unit direction. Then, this discrepancy must be due to differences in the mirror support between the factory (GP report) and Kryoneri (CCD out-of-focus images) support mount.

It is possible to make an estimate of the deformation of the mirror surfaces that is required to change the sign of spherical aberration between that predicted from the mirror prescription and what has been measured on the telescope. Positive spherical aberration (measured from the out of focus images) means that the rays from the outermost edge of the mirror come to focus first, and thus the outer edge of the mirror is higher than it should be, with respect to its centre. This means, that the spherical aberration can be changed from negative to positive, by raising the edge of the primary mirror. This change will be of the order of 3-4 microns at the edge of the mirror. This would change the wavefront error from the edge of the telescope aperture by about 11 wavelengths, going from ~-6 waves of negative spherical aberration to +5 waves of positive spherical aberration.

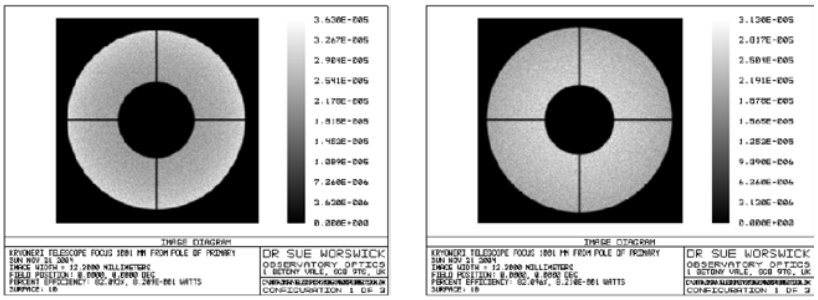

Figure 2. Extra focal image (left) and Intra focal image (right)

Table 4.

Position angle on image	DI pixels	Di pixels	DE pixels	de pixels	ΔD pixels	ΔD mm	Image diameter mm	Image diameter arcsec
0°	98.10	213.15	91.10	216.15	8.26	0.397	0.147	1.87
45°	99.05	212.60	90.71	215.50	9.56	0.459	0.170	2.16
90°	101.10	212.30	90.14	215.20	12.17	0.584	0.217	2.75
135°	99.60	212.80	90.84	215.70	9,98	0.479	0.178	2.26
Mean						0.479		2.25
SD						0.078		0.37

6. Image quality on the telescope's CCD

The diagram shows the image profiles produced when a spherical aberration image, refocused for minimum image spread, and with a 100% EE diameter of 2.25″ is convolved with a Gaussian profile ("seeing"). It can be seen that the effects of spherical aberration dominate the image spread under sub-second seeing. The image broadening imposed by the spherical aberration present in the Kryoneri telescope optics will lead to a pessimistic assessment of the seeing conditions at the site, as confirmed from DIMM tests (Mislis et al. 2005). The table below shows exactly how the spherical aberration dominates the "seeing" disk. Even at 2 arcsecond "seeing" the FWHM broadening factor is 1.23 times.

It can be seen that the spherical aberration distorts the Gaussian profile. If, instead of direct measurement, the FWHM of the convolved profile is estimated using Gaussian fitting, the following results are obtained (which only deviate by 30% from the results in table 5 under conditions of very good seeing where the profile strongly deviates from the Gaussian form):

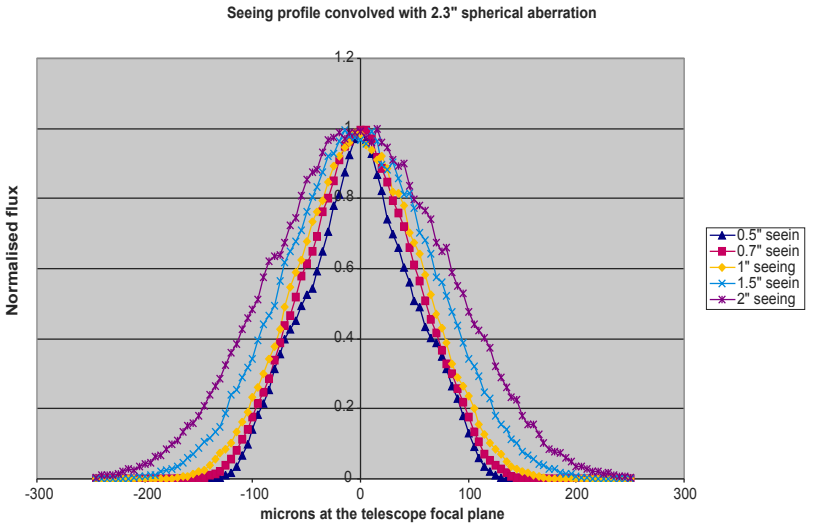

Figure 5.

Table 5

Image spread from convolution of seeing with spherical aberration					
Seeing FWHM ″	**0.5**	**0.7**	**1.0**	**1.5**	**2.0**
Image FWHM μm	106	122	136	162	195
Image FWHM ″	**1.34**	**1.54**	**1.72**	**2.04**	**2.45**
Broadening factor	2.68	2.2	1.72	1.36	1.23

Image spread obtained from Gaussian fitting to convolved profile					
Seeing FWHM ″	**0.5**	**0.7**	**1.0**	**1.5**	**2.0**
1-sigma μm	51	54	59	70	84
Image FWHM μm	120	127	139	165	197
Image FWHM ″	1.51	1.6	1.75	2.08	2.48
Broadening factor	3.02	2.28	1.75	1.39	1.24

Summary and conclusions

1. The manufacturing specification for the telescope secondary mirror is not consistent with correction of spherical aberration at the focus position used on the telescope.
2. Using the parameters within the GP mirror prescription and the current measured image position (1001 mm from the front surface of the primary mirror) the f-number is f/13.6 (focal length 16360 mm) and the image spread from spherical aberration would be 100% encircled energy within 2.6 arcseconds.
3. Previous measurements of the telescope image scale, undertaken by Synachopoulos et al., give a value of 0.301″ per 24-micron pixel. The calculated telescope focal length (cited in 2 above) gives an image scale of 0.0793 mm per arcsecond or 0.303″ per 24-micron pixel. This good agreement between calculated and measured image scale means that the focal lengths for the primary and secondary mirrors given in the GP report are correct.
4. The out-of-focus CCD images taken with the telescope show the presence of spherical aberration with 100% encircled energy within 2.25±0.37 arcseconds. However the sign of the spherical aberration measured derived from the CCD images is opposite to that within the factory telescope prescription. This discrepancy could be explained by a deformation of the primary mirror on its support.
5. The image quality from mirror polishing errors gives 95% encircled energy within 0.49 arcseconds and thus, the telescope performance is dominated by spherical aberration rather than "site seeing" or mirror polishing errors.

References

Grubb Parsons, "Optical test Reports", 1975

Mislis, D., Harlaftis, E.T., Buckley, D., Gazeas, K., Stathoulis, K., Dimou, G., Seiradakis, J.-H., 2005, "A test of Kryoneri "seeing" with DIMM equipment", Hipparchos, this issue

Rovithis, et al. 1999, Proceedings of "Astronomy 2000+ : Greek prospects for the 21st century", eds. E. Kontizas, R. Korakitis, J. Ventura, Greek National Committee for Astronomy, p. 138

Sinachopoulos, D., Dapergolas, A., van Dessel, E., Kontizas, E., "CCD astrometry and instrumental ΔV photometry of visual double stars", 1999, A & A SS, 136, 525

Wilson, R.N., "Reflecting Telescope Optics Manufacture, Testing, Alignment and Modern Techniques", 1999, Springer-Verlag Berlin, Heidelberg (ISBN: 3540603565)